Anal. Chem. **2009,** *81,* 1638–1645

Detection of Glucose Based on Direct Electron Transfer Reaction of Glucose Oxidase Immobilized on Highly Ordered Polyaniline Nanotubes

Ziyi Wang, Shuna Liu, Ping Wu, and Chenxin Cai*

Jiangsu Key Laboratory of Biofunctional Materials, College of Chemistry and Environmental Science, Nanjing Normal University, Nanjing 210097, P. R. China

An amperometric glucose biosensor based on the direct electron transfer of glucose oxidase (GOx) was developed by electrochemically entrapping GOx onto the inner wall of highly ordered polyaniline nanotubes (nanoPANi), which was synthesized using anodic aluminum oxide (AAO) membrane as a template. The cyclic voltammetric results indicated that GOx immobilized on the nanoPANi underwent direct electron transfer reaction, and the cyclic voltammogram displayed a pair of well-defined and nearly symmetric redox peaks with a formal potential of −405 ± 5 mV and an apparent electron transfer rate constant of 5.8 ± 1.6 s^{-1}. The biosensor had good electrocatalytic activity toward oxidation of glucose and exhibited a rapid response (~3 s), a low detection limit (0.3 ± 0.1 μM), a useful linear range (0.01−5.5 mM), high sensitivity (97.18 ± 4.62 μA mM^{-1} cm^{-2}), higher biological affinity (the apparent Michaelis−Mentan constant was estimated to be 2.37 ± 0.5 mM) as well as good stability and repeatability. In addition, the common interfering species, such as ascorbic acid, uric acid, and 4-acetamidophenol, did not cause any interference due to the use of a low detection potential (−0.3 V vs SCE). The biosensor can also be used for quantification of the concentration of glucose in real clinical samples.

Glucose detection is of practical importance in the food and fermentation analysis, in the textile industry, in environmental monitoring, and in medical diagnosis, etc.[1−3] Much effort has been focused on developing suitable techniques for precisely monitoring the glucose level with high sensitivity, high reliability, fast response, good selectivity, and low cost. Those approaches involve a surface plasmon resonance biosensor,[4] near-infrared optical biosensor,[5] capacitive detection,[6] electrochemiluminescene,[7] fluorescence detection,[8] colorimetry,[9] and amperometric biosensor, etc.[1,10−12] Among all methods, amperometric glucose biosensor is a promising method since it has the advantages of high sensitivity, compatibility for miniaturization, easy operation, and low cost.

Amperometric glucose biosensors are usually based on glucose dehydrogenase (GDH)[13] or glucose oxidase (GOx).[10,14,15] The nonenzymatic glucose detection based on nanomaterials is also reported. Those nanomaterials included copper nanocluster,[16] platinum nanoparticles,[17] carbon nanotube,[18] and dendritic platinum nanoparticles, etc.[19] However, the nonenzymatic glucose detection is usually performed in alkaline media with a high detection potential (usually 0.5−0.65 V, vs SCE),[16,19] and moreover, the sensitivity and detection limit of nonenzymatic glucose sensors are not as good as those of enzyme-based glucose sensors. The GDH-based biosensors involve the electrochemistry of NADH (reduced form of β-nicotinamide adenine dinucleotide). The biosensing of glucose requires a highly sensitive NADH transducer because the signal of the biosensor is based on the detection of the anodic current of enzymatically generated NADH.[13] Therefore, this kind of biosensor requires the addition of the soluble NAD^+ cofactor for enzymatic activity, which complicates the analysis system. Moreover, the direct oxidation of NADH at unmodified electrodes is not straightforward and requires high overpotential (usually 0.7−1.0 V) owing to the sluggish electron transfer kinetics.[20] The GOx-based glucose biosensor

* Corresponding author. E-mail: cxcai@njnu.edu.cn.

(1) Lee, S.-R.; Lee, Y.-T.; Sawada, K.; Takao, H.; Ishida, M. *Biosens. Bioelectron.* **2008**, *24*, 410–414.
(2) Newman, J. D.; Turner, A. P. F. *Biosens. Bioelectron.* **2005**, *20*, 2435–2453.
(3) Wu, L.; Zhang, X.; Ju, H. *Biosens. Bioelectron.* **2007**, *19*, 141–147.
(4) Shen, X. W.; Huang, C. Z.; Li, Y. F. *Talanta* **2007**, *72*, 1432–1437.
(5) Song, C.; Pehrsson, P. E.; Zhao, W. *J. Mater. Res.* **2006**, *21*, 2817–2823.
(6) Cheng, Z.; Wang, E.; Yang, X. *Biosens. Bioelectron.* **2001**, *16*, 179–185.
(7) Kremeskotter, J.; Wilson, R.; Schiffrin, D. J.; Luff, B. J.; Wilkinson, J. S. *Meas. Sci. Technol.* **1995**, *6*, 1325–1328.
(8) Barone, P. W.; Parker, R. S.; Strano, M. S. *Anal. Chem.* **2005**, *77*, 7556–7562.
(9) Morikawa, M.; Kimizuka, N.; Yoshihara, M.; Endo, T. *Chem.—Eur. J.* **2002**, *8*, 5580–5584.
(10) Du, P.; Zhou, B.; Cai, C. X. *J. Electroanal. Chem.* **2008**, *614*, 149–156.
(11) Kandimalla, V. B.; Tripathi, V. S.; Ju, H. *Biomaterials* **2006**, *27*, 1167–1174.
(12) Xian, Y.; Hu, Y.; Liu, F.; Xian, Y.; Feng, L.; Jin, L. *Biosens. Bioelectron.* **2007**, *22*, 2827–2833.
(13) Du, P.; Wu, P.; Cai, C. X. *J. Electroanal. Chem.* **2008**, *624*, 21–26.
(14) Jia, W.-Z.; Hu, Y.-K.; Song, Y.-Y.; Wang, K.; Xia, X.-H. *Biosens. Bioelectron.* **2008**, *23*, 892–898.
(15) Kohma, T.; Oyamatsu, D.; Kuwabata, S. *Electrochem. Commun.* **2007**, *9*, 1012–1016.
(16) Kang, X.; Mai, Z.; Zou, X.; Cai, P.; Mo, J. *Anal. Biochem.* **2007**, *363*, 143–150.
(17) Rong, L.-Q.; Yang, C.; Qian, Q.-Y.; Xia, X.-H. *Talanta* **2007**, *72*, 819–824.
(18) Ye, J.-S.; Wen, Y.; Zhang, W. D.; Gan, L. M.; Xu, G. Q.; Sheu, F.-S. *Electrochem. Commun.* **2004**, *6*, 66–70.
(19) Shen, Q.; Jiang, L.; Zhang, H.; Min, Q.; Hou, W.; Zhu, J.-J. *J. Phys. Chem. C* **2008**, *112*, 16385–16392.
(20) Meng, L.; Wu, P.; Chen, G.; Cai, C. X. *J. Electrochem. Soc.* **2008**, *155*, F231–F236.

10.1021/ac802421h CCC: $40.75
Published on Web 01/26/2009

catalyzes the oxidation of glucose to gluconolactone in the presence of oxygen, producing H_2O_2 simultaneously.[14,15] Quantification of glucose is achieved via electrochemical oxidation of the liberated H_2O_2. However, the oxidation of H_2O_2 usually requires a relatively high positive potential (usually over +0.6 V, vs SCE).[15,21] Many other electroactive species commonly coexisting in the biological fluids, such as ascorbic acid (AA), uric acid (UA), and 4-acetamidophenol (AP), can also be oxidized at the high potential and their electrochemical signals thus severely affect the selectivity of the biosensors. Therefore, interference elimination represents a main task to be solved for this type of biosensors. The interference can be partially overcome by coating the biosensor with a membrane impermeable to interfering agents[22] or oxidizing the interfering agents before they reach the biosensor.[23] However, coating with polymeric films leads to lower signals and longer response time due to the additional diffusion barrier, whereas using electrochemical preoxidation displays a risk of oxidizing the substrate of interest.

Alternatively, glucose can be detected based on the direct electron transfer (DET) of GOx without addition of any mediators or cofactors into the system. Although several papers have achieved the well-defined voltammetric peaks of DET of GOx,[24−26] there are few papers reporting the detection of glucose based on the DET of GOx. The GOx still needed mediators (such as O_2,[27−31] ferrocene monocarboxylic acid[24,25,32]) to catalyze the oxidation of glucose in those studies. Here, we report an example of the detection of glucose based on the DET of GOx by entrapping the enzyme in the inner wall of the highly ordered polyaniline nanotubes (nanoPANi).

The use of conducting polymers as sensing electrodes has attracted great interest because they exhibit a wide range of novel electrochemical properties.[33−38] Among all the conducting polymers, the one studied most is polyaniline, which has been studied extensively as an important conducting material that possesses interesting electrical, electrochemical, and optical properties.[39−42] Advantages of utilizing polyaniline in biosensors fabrication are impressive signal amplification and elimination of electrode fouling.[43] The polymer also provides a suitable environment for immobilization of biomolecules.[43] Recently, considerable efforts have been made on the synthesis of 1D nanostructured polyaniline because it displays unique properties which are significantly different from those of bulk films.[40,44−46] Although there were several reports on the synthesis of the polyaniline nanofiber, few papers reported the preparation of the ordered nanoPANi. In this work, the highly ordered nanoPANi was fabricated by employing anodic aluminum oxide (AAO) as a template. A glucose biosensor (GOx-nanoPANi) based on the DET of GOx was developed by electrochemically entrapping GOx into the inner wall of the nanoPANi. The characteristics of DET and electrocatalytic features of the immobilized GOx are presented. The proposed biosensor exhibits the advantages of ease of construction, enhanced electrocatalysis, efficiently preservation of the activity of enzyme, and effective discrimination to the common interfering species.

EXPERIMENTAL SECTION

Chemicals. GOx (EC 1.1.3.4, from *Aspergillus niger*, ~200 U/mg, Sigma), β-D-(+)-glucose (Sigma), ascorbic acid (AA), uric acid (UA), and 4-acetamidophenol (AP) were used as received. Prior to use, aniline was distilled under reduced pressure and stored in the dark. All other chemicals were of analytical grade. Phosphate buffer solution (PBS, 0.1 M, pH 5.5) was made up from Na_2HPO_4 and NaH_2PO_4. Solutions of GOx, AA, UA, and AP were prepared using PBS immediately before each experiment. The glucose stock solution was allowed to mutarotate for at least 24 h before use.

Fabrication of Ordered NanoPANi and Immobilization of GOx. The overall procedure of fabrication of ordered nanoPANi and immobilization of GOx is illustrated in Scheme 1. The AAO membrane with the pores size of 200−250 nm in diameter and the average interpore distance of 100 nm, which was prepared with the procedures described previously,[47] was used for the synthesis of the ordered nanoPANi. First, one side of the AAO membrane was coated with a layer of platinum film with thickness of ~10 nm by high-vacuum evaporation to serve as a working electrode (step a). The electrical contact was made to the Pt-coated AAO membrane using copper wire via conductive epoxy (Kunmin Institute of Noble Metals, Kunmin, China). Then Pt film and the copper wire were coated with a layer of insulating epoxy to avoid contact of solution with them. After that, the working electrode (denoted as the AAO/Pt electrode) was subjected to repeating potential scanning in 0.5 M H_2SO_4 solution containing 0.2 M aniline in the range of −0.4 to 1.0 V (step b). During the

(21) Shan, D.; Zhu, M.; Xue, H.; Cosnier, S. *Biosens. Bioelectron.* **2007**, *22*, 1612–1617.
(22) Scuvalio, O.; Soldatkin, O.; Lefebvre, A.; Cespuglio, R.; Soldatkin, A. *Anal. Chim. Acta* **2006**, *573*, 110–116.
(23) Cui, G.; Kim, S. J.; Choi, S. H.; Nam, H.; Cha, G. S. *Anal. Chem.* **2000**, *71*, 1925–1929.
(24) Cai, C. X.; Chen, J. *Anal. Biochem.* **2004**, *332*, 75–83.
(25) Liu, X.; Shi, L.; Niu, W.; Li, H.; Xu, G. *Biosens. Bioelectron.* **2008**, *23*, 1887–1890.
(26) Yang, T.-H.; Hung, C.-L.; Ke, J.-H.; Zen, J.-M. *Electrochem. Commun.* **2008**, *10*, 1094–1097.
(27) Zhang, Y.; Shen, Y.; Han, D.; Wang, Z.; Song, J.; Li, F.; Niu, L. *Biosens. Bioelectron.* **2007**, *23*, 438–443.
(28) Zhou, M.; Shang, L.; Li, B.; Huang, L.; Dong, S. *Biosens. Bioelectron.* **2008**, *24*, 442–447.
(29) Deng, C.; Chen, J.; Chen, X.; Xiao, C.; Nie, L.; Yao, S. *Biosens. Bioelectron.* **2008**, *23*, 1272–1277.
(30) Liu, S.; Ju, H. *Biosens. Bioelectron.* **2003**, *19*, 177–183.
(31) Forzani, E. S.; Zhang, H.; Nagahara, L. A.; Amiani, I.; Tsui, R.; Tao, N. *Nano Lett.* **2004**, *4*, 1785–1788.
(32) Wu, X.; Du, P.; Wu, P.; Cai, C. X. *Electrochim. Acta* **2008**, *54*, 738–743.
(33) Gregg, B. A.; Heller, A. *J. Phys. Chem.* **1991**, *95*, 5976–5980.
(34) Quinn, C. A. P.; Connor, R. E.; Heller, A. *Biomaterials* **1997**, *18*, 1665–1670.
(35) Yon-Hin, B. F. Y.; Smolander, M.; Crompton, T.; Lowe, C. R. *Anal. Chem.* **1993**, *65*, 2067–2071.
(36) Pishko, M. V.; Katakis, I.; Lindquist, S.-E.; Ye, L.; Gregg, B. A.; Heller, A. *Angew. Chem., Int. Ed.* **1990**, *29*, 82–84.
(37) Eng, L. H.; Elmgren, M.; Komlos, P.; Nordling, M.; Lindquist, S.-E.; Neujahr, H. Y. *J. Phys. Chem.* **1994**, *98*, 7068–7072.
(38) Csöregi, E.; Quinn, C. P.; Schmidtke, D. W.; Lindquist, S.-E.; Pishko, M. V.; Ye, L.; Katakis, I.; Hubbell, J. A.; Heller, A. *Anal. Chem.* **1994**, *66*, 3131–3138.
(39) Mathebe, N. G. R.; Morrin, A.; Iwuoha, E. I. *Talanta* **2004**, *64*, 115–120.
(40) Shi, L.; Xiao, Y.; Willner, I. *Electrochem. Commun.* **2004**, *6*, 1057–1060.
(41) Chen, Y.-H.; Wu, J.-Y.; Chung, Y.-C. *Biosens. Bioelectron.* **2006**, *22*, 489–494.
(42) Wang, H.; Mu, S. *J. Electroanal. Chem.* **1997**, *436*, 43–48.
(43) Sangodkar, H.; Sukeerthi, S.; Srinivasa, R. S.; Lal, R.; Contractor, A. Q. *Anal. Chem.* **1996**, *68*, 779–783.
(44) Huang, H.; Feng, X.; Zhu, J.-J. *Nanotechnology* **2008**, *19*, 145607–145613.
(45) Qiang, J.; Yu, Z.; Wu, H.; Yun, D. *Synth. Met.* **2008**, *158*, 544–547.
(46) Mi, H.; Zhang, X.; Yang, S.; Ye, X.; Luo, J. *Mater. Chem. Phys.* **2008**, *112*, 127–131.

Scheme 1. Schematic Diagram of Synthesis of Ordered Polyaniline Nanotube Using the AAO Membrane As a Template and Electrochemically Entrapping GOx on the Inner Wall of the Polyaniline Nanotube

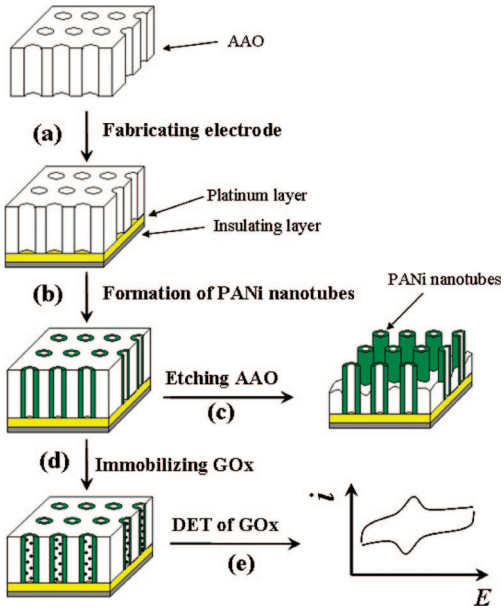

potential scanning, the electropolymerization of aniline occurred in the pore of the AAO membrane and the nanoPANi was formed. Extra care has to be taken, and the polymerizing cycles have to be optimized in order to obtain the nanoPANi without overgrowing of the polyaniline film on the surface of the AAO membrane. Usually, eight cycles of potential scanning at a scan rate of 50 mV/s were selected to synthesize the ordered nanoPANi of high quality.

For immobilization of GOx, several parameters were optimized to obtain the high performance of the prepared biosensor. Typically, the nanoPANi was first reduced in PBS (pH 5.5) at −250 mV for 15−20 min until a steady state was achieved in order to remove anions in the nanoPANi as completely as possible. Enzyme immobilization was achieved by oxidizing the reduced nanoPANi in PBS (containing 7 mg/mL of GOx) under a potential of +750 mV for 20 min (step d). During the oxidation process, negatively charged GOx (p*I* is 4.2[48]) were electrostatically entrapped onto the inner wall of nanoPANi. The resulted electrode was denoted as the GOx-nanoPANi/Pt electrode and was rinsed with doubly distilled water to remove any loosely entrapped enzyme. After that, the DET characteristics and electrocatalytic features of GOx were evaluated by voltammetry (step e). The electrode was stored in buffer at 4 °C when it was not in use.

In order to compare the significance of the nanotubes on immobilization of GOx, another electrode with a thin film of polyaniline was prepared on a Pt electrode under similar conditions to that of the GOx-nanoPANi/Pt electrode. The electrode was denoted as GOx-PANi/Pt.

Apparatus and Procedures. SEM images were recorded using a JEOL JSM-5610LV scanning electron microscope (Japan). To obtain the SEM images of nanoPANi, a thin layer of AAO membrane was etched away using 6 M NaOH (step c). The UV−vis spectra were recorded using a Cary 5000 UV−vis-NIR spectrophotometer (Varian). FT-IR spectra were recorded on a Nexus 670 FT-IR spectrophotometer (Nicolet Instruments) in a reflection mode.

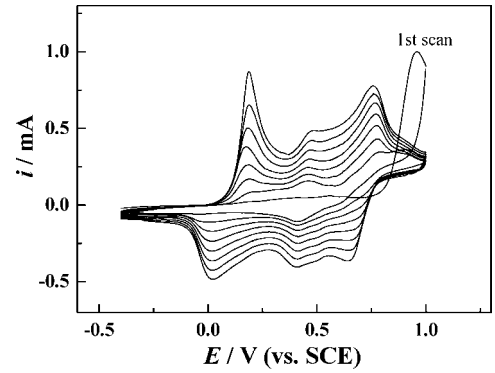

Figure 1. Cyclic voltammograms for the synthesis of polyaniline nanotube in the pores of the AAO membrane recorded in a 0.5 M H_2SO_4 solution containing 0.2 M aniline. The scan rate is 50 mV/s.

The electrochemical experiments were performed with a CHI 660B electrochemical workstation (CH Instruments). A two-compartment three-electrode cell with a sample volume of 10 mL was employed. A coiled Pt wire and a saturated calomel electrode (SCE) were used as the counter electrode and the reference electrode, respectively. The buffer was purged with high-purity nitrogen for at least 30 min prior to each electrochemical measurement, and the nitrogen environment was then kept over the solution to protect the solution from oxygen. Amperometric detection was performed under an applied potential of −0.3 V. The solution was continuously stirred using a magnetic bar at a speed of 250 rpm. A higher speed leads to increase of noise while a lower speed results in a longer responsive time. Therefore, it is better to choose an appropriate stirring speed of 250 rpm to obtain a good single-to-noise ratio and a short responsive time. The response was taken as the change between the steady state and background currents. All electrochemical experiments were performed at (40 ± 1) °C.

RESULTS AND DISCUSSION

Characterization of Polyaniline Nanotubes. When the AAO/Pt electrode was subjected to potential scanning in the range of −0.4 to 1.0 V in an acidic medium of aniline, aniline could be oxidized and polymerized in the pores of the AAO membrane. Initially, oxidation of aniline occurs at approximately +950 mV resulting in the nucleation of polyaniline. During subsequent scans, the oxidation of aniline takes place at lower potential due to the catalytic effect of polyaniline, which results in deposition of the polymer on the inner wall of AAO. An increase in the amplitude of redox peaks is observed as a consequence of repeated potential scans (Figure 1), indicating that the polymer has been deposited and confirming that the polyaniline is conducting.

The formation of nanoPANi was verified by SEM morphologies. Figure 2a is a typically top-view SEM image of the empty AAO membrane. It can be seen that the AAO has a highly ordered pore arrangement with a diameter of 250−300 nm and the average interpore distance of ∼100 nm. After the deposition of polyaniline, the diameter of the pores apparently decreases (∼150 nm), while the thickness of the interpore increases (∼200 nm, Figure 2b). This result suggests that nanoPANi has been formed along the inner walls

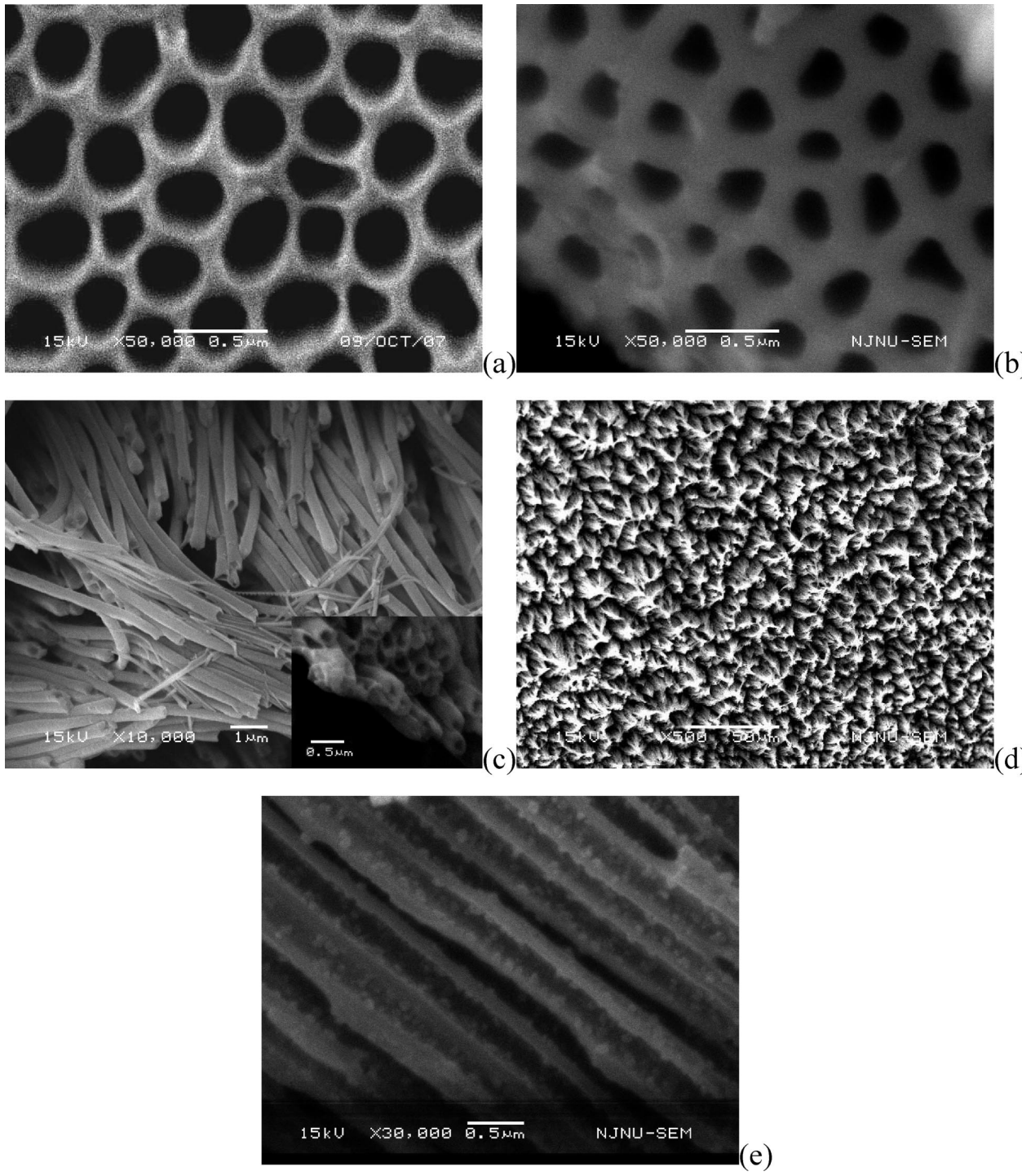

Figure 2. Typical SEM image of the AAO membrane before (a) and after (b) formation of polyaniline nanotube in the pores of the template. The SEM images of polyaniline nanotube obtained by etching away the AAO membrane (c and d). The cross-sectional image of the polyaniline nanotube after loading GOx on the inner wall of the nanotube (e).

of the pores of AAO. In order to observe the morphology of nanoPANi clearly, the AAO membrane was partially etched away using NaOH solution. Figure 2c shows that the nanotubes are highly ordered arranged with the outer diameter of 250−300 nm, which corresponds well to the diameter of the pores of AAO (Figure 2a). The open end of these nanotubes can be viewed clearly from the top-view SEM image (the inset of Figure 2c). The inner diameter of the nanotubes is ~150 nm, which is in good agreement with that viewed from Figure 2b. It should be noted that the highly ordered nanoPANi can be prepared on a large scale as indicated by the SEM picture at low magnification (Figure 2d).

The UV−vis and FT-IR spectra were also recorded to characterize the structure of the nanotubes (Figure 3). The results indicate that the nanotubes have similar spectroscopic characteristics with those of polyaniline film. The UV−vis spectrum shows that polyaniline nanotubes exhibit three

(47) Shi, Y.; Zhou, B.; Wu, P.; Wang, K.; Cai, C. X. *J. Electroanal. Chem.* **2007**, *611*, 1–9.

(48) Kim, K. K. A.; Fravel, D. R.; Papavizas, G. C. *Can. J. Microbiol.* **1990**, *36*, 760–764.

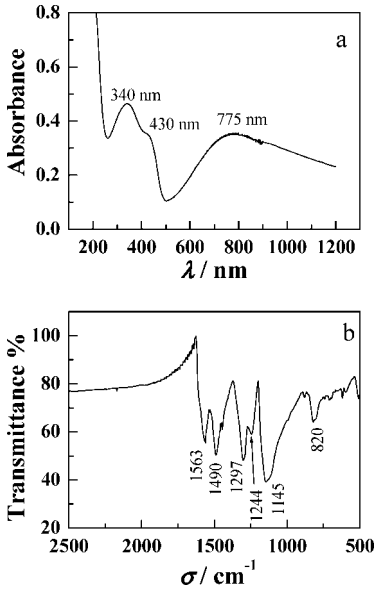

Figure 3. The UV−vis (a) and FT-IR (b) spectra of the prepared polyaniline nanotube.

absorption peaks at 340, 430, and 775 nm (Figure 3a), which are the characteristic absorption peaks of the emeraldine oxidation state of polyaniline.[46] The absorption peaks at 340 and 430 nm are attributed to the $\pi^*-\pi$ transition of benzenoid rings and polaronic peak, reflecting protonation of backbone of the nanotubes. The peak at 775 nm represents the $\pi-$polaron transition, indicating that the nanotubes are in the conductive state.[49] In the FT-IR spectrum represented in Figure 3b, the peaks at 1563 and 1490 cm^{-1} belong to the C=C stretching of the quinoid ring and benzenoid ring, respectively. Those at 1297 and 1145 cm^{-1} are attributed to C−N stretching of the secondary aromatic amine. The peak at 820 cm^{-1} is ascribed to the out-of-plane bending of C−H on the 1,4-disubstituted ring. The peak at 1244 cm^{-1} can be attributed to various stretching and bending associated with the C−C bond.[50] The band at 1145 cm^{-1} was referred to as the "electronic-like band", and its intensity was considered as a measure of the degree of delocalization of electrons on polyaniline.[51] Therefore, it is a characteristic peak of polyaniline conductivity. The high intensity of this peak suggests that the conductivity of the synthesized polyaniline nanotube is high. This feature suggests that the nanotubes can be used as an electrode matrix for electrochemical investigation.

The nanotubes produced in this work provide an ideal size of channel to entrap the GOx since the particle size of GOx is in the range of 10−100 nm.[52] Moreover, the nanotube structure can significantly increase the effective surface for the loading enzyme and accelerate electron transfer. After GOx was entrapped into the nanotubes, some small and uniformly distributed islandlike nanostructures with the size of ~50 nm were adhered on the inner wall of nanoPANi (Figure 2e). These nanostructures are the aggregates of the entrapped GOx molecules, indicating the

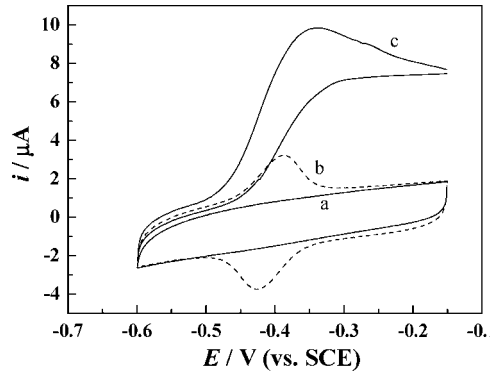

Figure 4. Cyclic voltammograms of the nanoPANi/Pt (a) and GOx-nanoPANi/Pt (b) electrodes in PBS (0.1 M, pH 5.5) in the absence of glucose. (c) Cyclic voltammogram of the GOx-nanoPANi/Pt electrode in PBS containing 5 mM glucose. Scan rate: 10 mV/s.

effective immobilization of the enzyme. This cross-sectional image was obtained by breaking the AAO membrane (GOx has been entrapped) arbitrarily since cutting the highly brittle membrane to obtain a planar cross section is difficult. It should be note that nanoPANi still retains the nanotube structure even after GOx was immobilized. This characteristic is very important when the GOx-nanoPANi is further used for sensing substrates (such as glucose) because the nanotube structure enables free and fast diffusion of substrates and products inside the nanotube.

Direct Electron Transfer of GOx and the Electrocatalytic Oxidation of Glucose. The cyclic voltammograms of the nanoPANi/Pt (a) and GOx-nanoPANi/Pt (b) electrodes in PBS (0.1 M, pH 5.5) are depicted in Figure 4. No redox peaks is observed at the nanoPANi/GC electrode (curve a), suggesting that nanoPANi cannot undergo the redox reaction in this potential range. However, the GOx-nanoPANi/GC electrode shows a pair of well-defined and nearly symmetrical redox peaks with the anodic and cathodic peak potentials at −390 and −420 mV (at 10 mV/s, curve b), respectively. The formal potential ($E^{0'} = -405 \pm 5$ mV) is independent of the scan rate ranging from 10 to 300 mV/s, agreeing with the previously reported results.[24−27] Therefore, the pair of peaks in curve b can be ascribed to the DET reaction (the conversion of $FAD/FADH_2$ center) of GOx. The separation of peak potentials (ΔE_p) is 30 mV, indicating that GOx on the inner wall of nanoPANi can display a quasi-reversible electrochemical reaction despite its large molecular structure. Both the anodic and cathodic peak currents increase linearly with the scan rate (not shown here). This result is in agreement with that expected by the theory of a surface-confined redox process, and it also confirms that the immobilized GOx is stable. The apparent electron-transfer rate constant (k_s) is estimated to be (5.8 ± 1.6) s^{-1} from the dependence of ΔE_p on the scan rates.[53] This value is much higher than those reported previously at a carbon nanotube electrode ($1.5-1.7$ s^{-1}),[24] at a boron-doped carbon nanotube electrode (1.56 s^{-1}),[29] and at a single-walled carbon nanohorns-based electrode (3.0 s^{-1}).[25] This result suggests that DET of GOx on the inner wall of nanoPANi has good reversibility. Moreover, the electrochemical characteristics of the GOx-nanoPANi/Pt electrode are fairly stable since the features of the cyclic voltammogram remain almost invariable after the electrode was scanned continuously

(49) Athawale, A. A.; Kulkarni, M. V.; Chabukswar, V. V. *Mater. Chem. Phys.* **2002**, *73*, 106–110.
(50) Kan, J.; Lv, R.; Zhang, S. *Synth. Met.* **2004**, *145*, 37–42.
(51) Tang, J.; Jing, X.; Wang, B.; Wang, F. *Synth. Met.* **1988**, *24*, 231–238.
(52) Shan, D.; He, Y.; Wang, S.; Xue, H.; Zheng, H. *Anal. Biochem.* **2006**, *356*, 215–221.
(53) Laviron, E. *J. Eletroanal. Chem.* **1979**, *101*, 19–28.

for a long time (~100 cycles, at 10 mV/s). In addition, no obvious change is detected after the electrode has been stored in PBS at 4 °C for 1 week.

To illustrate the special effects of the nanoPANi in facilitating DET of GOx, the enzyme was also electrochemically entrapped into the polyaniline film, which was formed on the surface of the Pt electrode (see Experimental Section). The results indicate that GOx-PANi/Pt electrode does not show any observable redox peak in the potential range of −0.6 to −0.15 V (not shown here), suggesting that GOx cannot undergo the DET reaction in the polyaniline film. The exact reason of effective promotion of the nanoPANi to DET of GOx is not fully understood. The special nanotube structure may play an important role in facilitating DET of GOx.

Upon the addition of the glucose (5 mM), the shape of the cyclic voltammogram of the GOx-nanoPANi/Pt electrode changes significantly and is characterized by a large anodic peak at ~−340 mV (Figure 4c); meanwhile, the cathodic peak disappears completely. The increase of glucose concentration leads to the enhancement of the anodic current. These characteristics are the typical features of electrocatalytic reactions. Control results showed that electrocatalytic oxidation of glucose did not occur at the nanoPANi/Pt electrode (without loading GOx). These results verify that the entrapped GOx does not undergo the denaturation and still keeps its intrinsic electrocatalytic activities toward its substrates. These results also suggest that the GOx-nanoPANi/Pt electrode can be used as a biosensor to sense glucose. The electrocatalytic processes can be depicted as follows:

$$\mathrm{GOx(FAD) + glucose \rightarrow GOx(FADH_2) + gluconolactone} \quad (1)$$

$$\mathrm{GOx(FADH_2) \rightarrow GOx(FAD) + 2e^- + 2H^+} \quad (2)$$

Optimizing the Parameters of the Biosensor Performance. The performance of the GOx-nanoPANi/Pt biosensor toward the oxidation of glucose can be affected by a variety of parameters, such as the amount of GOx loading, detection potential, pH of the buffer solution, and temperature of the system, etc. In this work, these conditions are optimized.

The concentration of GOx in PBS during the biosensor fabrication procedure may affect the loading amount of the enzyme. Therefore, the effects of the loading amount of GOx on the performance of the biosensor were investigated. The biosensor was constructed in various concentrations of GOx, and the response of the prepared biosensor toward the oxidation of 2.5 mM glucose was recorded. The results were presented in Figure 5a. Increasing the enzyme loading leads to an enhancement in the response current for the oxidation of glucose and the response reaches a maximum at the concentration of 7 mg/mL of GOx. The response of the biosensor has a slight decrease at a higher concentration of GOx (for example, 10 mg/mL). This decrease may be due to the blockage created by the GOx overloading in the channel of the PANi nanotube array. Therefore, the substrate and product cannot freely move into and out of the nanotube. The electron relaying capacity of the nanotube may also be disturbed because of the presence of the large amount of the insulating and bulky enzyme molecules. Therefore, a concentration of 7 mg/mL of GOx is chosen as the optimal concentration for construction of the biosensor.

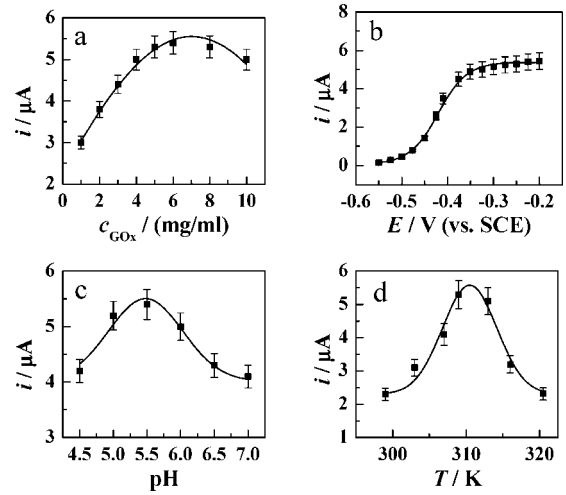

Figure 5. The dependence of the response of the GOx-nanoPANi/Pt biosensor toward the oxidation of 2.5 mM glucose on the amount of GOx loading (a), the detection potential (b), the pH of the buffer (c), and the temperature of the system (d). Every point is an average value of five independent measurements.

The choice of the detection potential is necessary to achieve the lowest detection limit and avoid the electrochemical interfering species. The response increases with the detection potential from −0.55 to −0.35 V and then reaches a plateau at higher potentials (Figure 5b). Thus, a detection potential of −0.3 V is selected. This potential is 900, 700, and 200 mV more negative than those used at the glucose biosensors by entrapping GOx into porous poly(acrylonitrile-*co*-acrylic acid) film (0.6 V),[52] polypyrrole film (0.4 V),[54] and Prussian blue nanostructures (0.1 V),[12] respectively. Please note that the detection of glucose is based on the oxidation of H_2O_2 in those studies; however, this study is based on the DET of GOx. The low detection potential will significantly diminish the influence of those easily oxidizable species.

A further optimized experimental parameter is the solution pH. In the range of pH variant from 4.5 to 7.0, an optimal response is found at approximately pH 5.5 (Figure 5c), which is in good agreement with the pH 5−6 reported for the native GOx in solution.[55] This result indicates that the immobilization procedure can keep the native activity of GOx. The temperature effect of the biosensor was evaluated between 25 and 50 °C. The response increases when the temperature rises from 25 to 40 °C, and the maximum response appears at approximately 40 °C (Figure 5d). At higher temperature, the response decreases due to the denaturation of the enzyme.

Amperometric Characteristics of the Biosensor. Figure 6a shows the amperometric response of the GOx-nanoPANi/Pt biosensor to the successive addition of glucose in solution under the optimal condition. Immediately after the addition of glucose, the response increases and reaches a steady state within ~3 s. The response time is similar to that obtained by immobilizing GOx on the surface of polypyrrole film (3 s).[54] However, it is lower than those obtained at other electrodes (see Table 1), suggesting that the electrode responds rapidly to the change of the substrate

(54) Ekanayake, E. M. I. M.; Preethichandra, D. M. G.; Kaneto, K. *Biosens. Bioelectron.* **2007**, *23*, 107–5005.
(55) Bright, H. J.; Appleby, M. *J. Biol. Chem.* **1969**, *244*, 3625–3634.

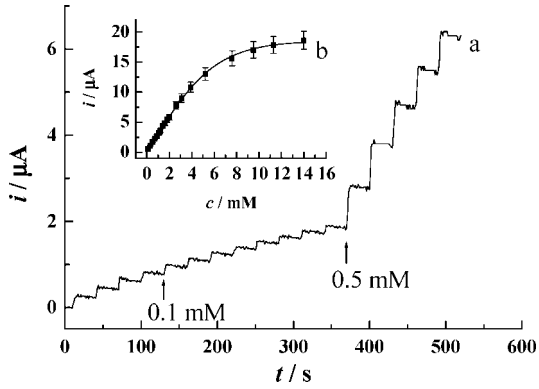

Figure 6. (a) Amperometric response of the GOx-nanoPANi/Pt biosensor to successive addition of glucose in PBS (0.1 M, pH 5.5) at an applied potential of −0.3 V. (b) Calibration curve for glucose obtained at the GOx-nanoPANi/Pt biosensor.

concentration. The electrode linearly responds to glucose at lower concentration and attains a saturation level at a higher concentration as expected by Michaelis−Menten type enzyme kinetics (Figure 6b). The apparent Michaelis−Menten constant (K_M^{app}) is estimated to be (2.37 ± 0.5) mM from the Lineweaver−Burk plot. The response displays a linear range from 0.01 to 5.5 mM with a correlation coefficient of 0.996 and a slope of 7.58 ± 0.36 μA mM^{-1}. Therefore, the sensitivity is calculated to be 97.18 ± 4.62 μA mM^{-1} cm^{-2}. The apparent surface of the electrode is estimated to be ∼0.078 cm^2 using the method reported previously.[56] The detection limit is estimated to be∼0.3 ± 0.1 μM at a signal/noise (S/N) of 3, which is much lower than those obtained at other electrodes (see Table 1).

From Table 1, one can conclude that the proposed biosensor has a higher sensitivity and a lower detection limit than those previous reported models. The high sensitivity implies that nanoPANi can provide a good biocompatible microenvironment for maintaining enzymatic activity. Moreover, the ordered nanoPANi formed in the AAO membrane can behave as an ensemble of closely spaced but isolated nanoelectrodes. Therefore, the S/N ratio can be greatly improved because the double layer charge current at nanoelectrode ensembles is orders of magnitude lower than that at a macroelectrode.[57] Therefore, a very low detection limit and high sensitivity are achieved when the ordered nanoPANi is used as a platform for glucose sensing. From Table 1, one can also conclude that the K_M^{app} value is quite low in comparison with those obtained at other glucose biosensors. This may be due to the favorable situation with low transport limitations of substrate, which are a result of the special spatial distribution of the nanoPANi nanotubes-immobilized enzymes. The good spatial distribution of enzymes leads to that the enzymes can be easily accessed by substrate molecules. This is an advantage of the proposed biosensor compared with those reported previously.

Different aspects regarding the characteristics of the biosensor are evaluated. The RSD (relative standard deviation) is ∼2.8% estimated from slopes of calibration plots for five different and freshly prepared electrodes, revealing an acceptable repeatability in the construction of the electrode. The assay precision of the biosensor was examined by five determinations at a glucose concentration of 2 mM. A RSD of ∼3.3% is obtained. Also, the stability of the electrode is considered. When the biosensor was not in use, it was stored in buffer at 4 °C. Its response to 2 mM glucose was recorded at a 1−2 day interval. The response decreases slightly in the initial few days (∼3 days), and afterward the response tends to be practically constant and can still retain ∼91% of its original response even after 2 weeks' storage. Even after the biosensor has been used continually for 1 week (two measurements a day), its response still remains at ∼88% of the initial value. Another attractive feature of the biosensor is that the response can still retain ∼90% of its original signal even after the biosensor is under extended polarization at −0.3 V for 6 h in a stirred solution of 2 mM glucose (Figure 7a). This means that the biosensor can be used as a stable sensor for glucose detection. The high stability can be attributed to the capability of entrapping GOx molecules and the good biocompatibility of the nanotubes retaining their biological activities. This improved stability may also be attributed to the special structure of the nanotubes, which is beneficial for the substrates to get access to the enzyme molecules. In addition, the fast diffusion of species from nanotubes and the effective protection of enzyme from leaking from the nanotubes may also contribute to the improvement in the stability of the biosensor.

In real samples, there are some coexisting electroactive species, for example, AA, UA, and AP, etc., might affect the biosensors response. The selectivity and anti-interference advantages of the biosensor are demonstrated (Figure 7b). While a well-defined glucose response is observed at the biosensor, relevant physiological level of AA, UA, and AP (0.2 mM, respectively) results in negligible signals. This feature is largely attributed to the low operating potential used in the detection. Hence, a highly selective response to glucose is obtained without the use of a perm-selective membrane or enzymatic preoxidation. This is another advantage of the proposed biosensor over those reported previously.

Real Sample Analysis. To evaluate its applicability, the biosensor was used for determination of the concentration of glucose in human urine. Five urine samples obtained from hospital were analyzed by using five independently prepared biosensors (one biosensor for per sample). Only an appropriate dilution of the samples with the supporting electrolyte (PBS, pH 5.5) was needed before the measurements were performed. The determined results were compared with those provided by the hospital (Table 2). It is shown that the values measured by the proposed biosensor are in good agreement with the data provided by hospital, demonstrating the great potential for practical application of the biosensor for the analysis of glucose on real clinical samples.

(56) Du, P.; Liu, S.; Wu, P.; Cai, C. X. *Electrochim. Acta* **2007**, *52*, 6534–6547.
(57) Martin, C. R.; Mitchell, D. T. *Electroanalytical Chemistry*; Marcel Dekker: New York, 1999; Vol. 21, p 18.
(58) Chen, X.; Jia, J.; Dong, S. *Electroanalysis* **2003**, *15*, 608–612.
(59) Salimi, A.; Compton, R. G.; Hallaj, R. *Anal. Biochem.* **2004**, *333*, 49–56.
(60) Uang, Y.; Chou, T. C. *Biosens. Bioelectron.* **2003**, *20*, 2435–2453.
(61) Zheng, H.; Xue, H.; Zhang, Y.; Shen, Z. *Biosens. Bioelectron.* **2002**, *17*, 541–545.
(62) Zhang, Z.; Liu, H.; Deng, J. *Anal. Chem.* **1996**, *68*, 1632–1638.
(63) Narang, U.; Prasad, P. N.; Bright, F. V. *Anal. Chem.* **1994**, *66*, 3139–3144.
(64) Vidal, J. C.; García, E.; Castillo, J. R. *Sens. Actuators, B* **1999**, *57*, 219–226.
(65) Gregg, B. A.; Heller, A. *Anal. Chem.* **1990**, *62*, 258–263.

Table 1. Comparison of Analytical Performance of Some Glucose Biosensors

glucose biosensor	sensitivity (μA mM^{-1} cm^{-2})	detection limit (μM)	response time (s)	K_M^{app} (mM)	ref
GOx-nanoPANi	97.18 ± 4.62	0.3 ± 0.1	~3	2.37 ± 0.5	this work
GOx-sol−gel-chitosan	0.274	10	<30	21 ± 1	58
GOx-sol−gel-CNTs[a]	0.2	50	5		59
GOx-polypyrrole	0.007		15	37.6	60
Nafion-GOx-OMC[b]	0.053	156.52	9 ± 1		28
Nafion-GOx-SWCNH[c]	1.06	6		8.5	25
GOx-Nb-SWNT[d]		10	5	4.6	13
GOx-PANAA[e]	6.82	0.5	<30	7.3	51
GOx-polyacrylonitrile	4.2	20	~20	14.4	61
GOx-poly(*o*-aminophenol)		0.5	4	16.4	62
GOx-TEOS-sol−gel[f]		200	30		63
GOx-PPy/*o*PPD[g]	0.019	5.14	5.1	22.7	64
GOx-redox polymer[h]			10	7.3	65

[a] CNT: carbon nanotube. [b] OMC: ordered mesoporous carbon. [c] SWCNH: single-walled carbon nanohorns. [d] Nb: nile blue. SWNT: single-walled carbon nanotube. [e] PANAA: porous poly(acrylonitrile-*co*-acrylic acid) film. [f] TEOS: tetraethyl orthosilicate. [g] PPy: polypyrrole. *o*PPD: poly(*o*-phenylenediamine). [h] The redox polmer is a cross-linkable poly(vinylpyridine) complex of $[Os(bpy)_2Cl]^{+/2+}$, bpy is bipyridine.

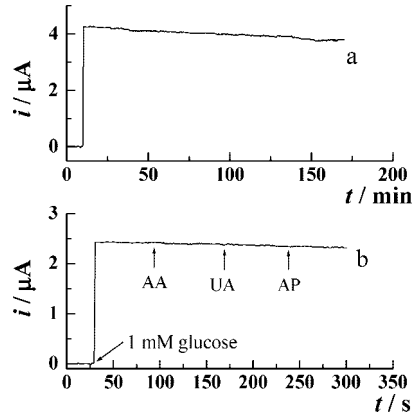

Figure 7. (a) Current traces illustrating the operational stability of the GOx-nanoPANi/Pt biosensor under continuous polarization and continuous exposure to a stirred solution of 2 mM glucose. (b) Amperometric responses of the biosensor upon additions of glucose (1 mM), AA (0.2 mM), UA (0.2 mM), and AP (0.2 mM) in PBS. The biosensor was biased on the potential of −0.3 V.

Table 2. Determination of Glucose Content in Urine Sample Using the GOx-nanoPANi/Pt Biosensor

no.	referenced values[a] (mM)	determined values[b] (mM)	relative deviation (%)
1	4.6 ± 0.12	4.5 ± 0.15	−2.2
2	4.8 ± 0.18	4.9 ± 0.11	2.1
3	5.1 ± 0.23	5.3 ± 0.28	3.9
4	7.8 ± 0.26	7.6 ± 0.24	−2.6
5	9.1 ± 0.32	9.4 ± 0.25	3.2

[a] Value provided by hospital. [b] Value determined by the GOx-nanoPANi/Pt biosensor; it is an average value of the response of five measurements for each sample.

CONCLUSIONS

In summary, a new glucose biosensor based on the direct electron transfer of GOx has been proposed by entrapping the GOx into a highly ordered polyaniline nanotube. The biosensor possesses rapid response, low detection limit with satisfactory stability, repeatability, and selectivity, and it can be used for detection of glucose content in clinical samples. The fabrication approach of the biosensor has advantages such as ease of construction, enhanced electrocatalysis, efficient preservation of the activity of the enzyme, and effective discrimination to the common interfering species.

ACKNOWLEDGMENT

This work is supported by the National Natural Science Foundation of China (Grants 20673057, 20773067, and 20833006) and the Program for New Century Excellent Talents in University (Grant NET-06-0508).

Received for review November 14, 2008. Accepted January 3, 2009.

AC802421H